Geophysical Research Letters

RESEARCH LETTER
10.1029/2018GL078374

Key Points:
- Crack-seal veins in subduction mélange record repeated low-angle thrust faulting under tensile overpressure
- The minimum time interval between thrusting events is comparable to recurrence intervals of slow earthquakes
- Crack-seal veins and viscous shear zones in subduction mélange may be geological manifestations of episodic tremor and slow slip

Supporting Information:
- Supporting Information S1
- Data Set S1

Correspondence to:
K. Ujiie,
kujiie@geol.tsukuba.ac.jp

Citation:
Ujiie, K., Saishu, H., Fagereng, Å., Nishiyama, N., Otsubo, M., Masuyama, H., & Kagi, H. (2018). An explanation of episodic tremor and slow slip constrained by crack-seal veins and viscous shear in subduction mélange. *Geophysical Research Letters*, *45*, 5371–5379. https://doi.org/10.1029/2018GL078374

Received 16 APR 2018
Accepted 22 MAY 2018
Accepted article online 29 MAY 2018
Published online 6 JUN 2018

An Explanation of Episodic Tremor and Slow Slip Constrained by Crack-Seal Veins and Viscous Shear in Subduction Mélange

Kohtaro Ujiie[1,2], Hanae Saishu[3,4], Åke Fagereng[5], Naoki Nishiyama[1], Makoto Otsubo[4], Haruna Masuyama[1], and Hiroyuki Kagi[6]

[1]Graduate School of Life and Environmental Sciences, University of Tsukuba, Tsukuba, Japan, [2]Research and Development Center for Ocean Drilling Science, Japan Agency for Marine-Earth Science and Technology, Yokohama, Japan, [3]Renewable Energy Research Center, National Institute of Advanced Industrial Science and Technology, Koriyama, Japan, [4]Geological Survey of Japan, National Institute of Advanced Industrial Science and Technology, Tsukuba, Japan, [5]School of Earth and Ocean Sciences, Cardiff University, Cardiff, UK, [6]Geochemical Research Center, Graduate School of Science, University of Tokyo, Tokyo, Japan

Abstract Episodic tremor and slow slip (ETS) occurs in the transition zone between the locked seismogenic zone and the deeper, stably sliding zone. Actual mechanisms of ETS are enigmatic, caused by lack of geological observations and limited spatial resolution of geophysical information from the ETS source. We report that quartz-filled, crack-seal shear and extension veins in subduction mélange record repeated low-angle thrust-sense frictional sliding and tensile fracturing at near-lithostatic fluid pressures. Crack-seal veins were coeval with viscous shear zones that accommodated deformation by pressure solution creep. The minimum time interval between thrusting events, determined from a kinetic model of quartz precipitation in shear veins, was less than a few years. This short recurrence time of low-angle brittle thrusting at near-lithostatic fluid overpressures within viscous shear zones may be explained by frequent release of accumulated strain by ETS.

Plain Language Summary Slow earthquakes have been detected from seismologic and geodetic observations. Episodic transfer of stress from slow earthquake source region to locked seismogenic zone is thought to trigger huge megathrust earthquakes. Despite these important findings and suggestions for slow earthquakes, actual conditions and underlying deformation mechanisms of slow earthquakes are still lacking. This paper reports that low-angle brittle thrusting at very small shear strength under near-lithostatic fluid overpressures repeatedly occurred at the time scale of slow earthquakes within viscous shear zones. This report is based on detailed geological study of the subduction mélange exposed in the Shimanto accretionary complex, southwest Japan, which is thought to be the on-land analogue of the Nankai Trough subduction zone. In the paper, we suggest that crack-seal shear and extension veins and localization of viscous shear are geological manifestation of episodic tremor and slow slip and represent frequent release of accumulated strain in the transition zone between the locked seismogenic zone and deeper, stably sliding zones. This will provide fundamental geological evidence for the mechanics and kinematics at the slow earthquake source and the possibility that this strain release could cause increased probability of triggering megathrust earthquakes in the seismogenic zone updip of this frequent loading.

1. Introduction

A spectrum of slow earthquake behaviors, including low-frequency tectonic tremors (LFTs), low-frequency earthquakes (LFEs), very LFEs (VLFEs), and slow slip events (SSEs), has been detected from seismologic and geodetic observations (Beroza & Ide, 2011; Obara & Kato, 2016; Peng & Gomberg, 2010; Saffer & Wallace, 2015; Schwartz & Rokosky, 2007). Tectonic tremor is defined as a persistent low-frequency seismic signal that lasts for days to weeks but is interpreted to represent a swarm of LFEs that accommodate shear slip on low-angle thrusts (Ide et al., 2007; Shelly et al., 2007). Slow slip is a geodetically detected, transient creep event where slip speed exceeds average plate motion but is too slow to generate detectable seismic waves. On some faults, SSEs appear to repeat near-periodically in the same location, and in some places, these events are spatiotemporally accompanied by LFTs, referred to as episodic tremor and slow slip (ETS; Obara et al., 2004; Rogers & Dragert, 2003).

In subduction zones, slow earthquake phenomena generally occur in transition zones between interseismically locked and stably sliding fault segments (Peng & Gomberg, 2010; Schwartz & Rokosky, 2007). ETS events are typically observed along the plate boundary thrust near the mantle wedge corner in relatively warm subduction zones. These events repeat at least every few years and thus lead to episodic transfer of stress from the ETS region to the locked seismogenic zone; this stress change may contribute to trigger megathrust earthquakes (Obara & Kato, 2016). Recent studies in the Nankai subduction zone have revealed that LFTs, LFEs, and SSEs occur along the plate boundary at depths of ~6–9 km and ~15 km (Araki et al., 2017; Nakano et al., 2018; Yamashita et al., 2015). The components of ETS can therefore be generated along the plate boundary at depths much shallower than the mantle wedge corner.

Despite the importance for understanding the dynamics of slow earthquakes and their relation to megathrust earthquakes, the underlying deformation mechanisms responsible for slow earthquake-generated deformation remain poorly understood. This shortfall in physical understanding arises from insufficient geological information on slow earthquakes, limited constraint on the temporal relationship between slow earthquakes and ordinary megathrust earthquakes, and poor spatial constraints on the source area of slow earthquakes and the spatiotemporal relation between tremor and slow slip. Whereas geological evidence for high-speed slip, such as pseudotachylyte (solidified frictional melt produced by seismic slip), has been reported from subduction zones (Ujiie et al., 2007; Ujiie & Kimura, 2014), low-speed deformation responsible for slow earthquakes has been attributed to brittle failure of relatively strong lenses coincident with viscous shear in surrounding matrix (Behr et al., 2018; Fagereng et al., 2014; Hayman & Lavier, 2014; Skarbek et al., 2012).

The exhumed Makimine mélange in the Late Cretaceous Shimanto accretionary complex of eastern Kyushu, southwest Japan (Figure 1), records progressive plate boundary deformation during subduction of young, warm oceanic crust to a shallow (10–15 km) frictional-viscous transition where temperatures reached 300–350°C (Hara & Kimura, 2008; Mackenzie et al., 1987; Palazzin et al., 2016). This mélange is exhumed from a frictional-viscous transition zone, typical of where slow earthquakes commonly occur. We examine the potential record of slow earthquakes by considering four key geophysical observations from active subduction margins (Araki et al., 2017; Beroza & Ide, 2011; Obara et al., 2004; Obara & Kato, 2016; Peng & Gomberg, 2010; Rogers & Dragert, 2003; Saffer & Wallace, 2015; Schwartz & Rokosky, 2007; Wallace et al., 2016): (1) Slow earthquakes typically occur in regions of high fluid pressure and low effective stress; (2) VLFEs, and triggered swarms of LFEs associated with SSEs, have very low stress drops (tens of kilopascal), implying that the effective fault strength is very weak and sensitive to perturbations; (3) when the focal mechanism is determined, slow earthquakes commonly exhibit shear slip on low-angle thrust faults subparallel to the plate boundary interface; and (4) ETS events repeat every several months to a few years.

2. Geological Setting

The Shimanto accretionary complex distributed along the Pacific side of southwest Japan has been believed to represent an ancient on-land analog of the Nankai Trough subduction zone (Figure 1a; Ujiie & Kimura, 2014). The Makimine mélange in the Shimanto accretionary complex of eastern Kyushu is Cenomanian to Campanian/Maastrichian in age (Late Cretaceous) and experienced prehnite-actinolite to greenschist facies metamorphism at 10–15 km depth (Hara & Kimura, 2008; Palazzin et al., 2016). The maximum temperatures determined from Raman spectra of carbonaceous material, vitrinite reflectance, and illite crystallinity range from 300 to 350°C (Hara & Kimura, 2008; Palazzin et al., 2016; supporting information). The mélange generally dips north-northwestward. The Makimine mélange preserves ocean plate stratigraphy composed, in ascending order, of (1) mudstone-dominated mélange containing basalt lenses and hemipelagic red mudstone at the base, (2) reddish brown tuff, and (3) sandstone-mudstone mélange and coherent turbidites (Figure 1b). This stratigraphy is repeated at least twice along the coastal exposure, possibly caused by duplex underplating after subduction, with the apparent thickness of each thrust sheet in the range 1,300–1,600 m. The subduction-related deformation at the frictional-viscous transition is well preserved (Mackenzie et al., 1987; Palazzin et al., 2016). Stretching lineations defined by aligned mica prisms, quartz rods, and long axes of sandstone blocks are particularly well developed in the structurally lower part of the mélange (Figure 1c). This lineation represents constrictional strain and is interpreted as parallel to the tectonic transport direction during subduction-related deformation and indicates that the subduction direction was perpendicular to the general strike of the mélange (Figure 1d).

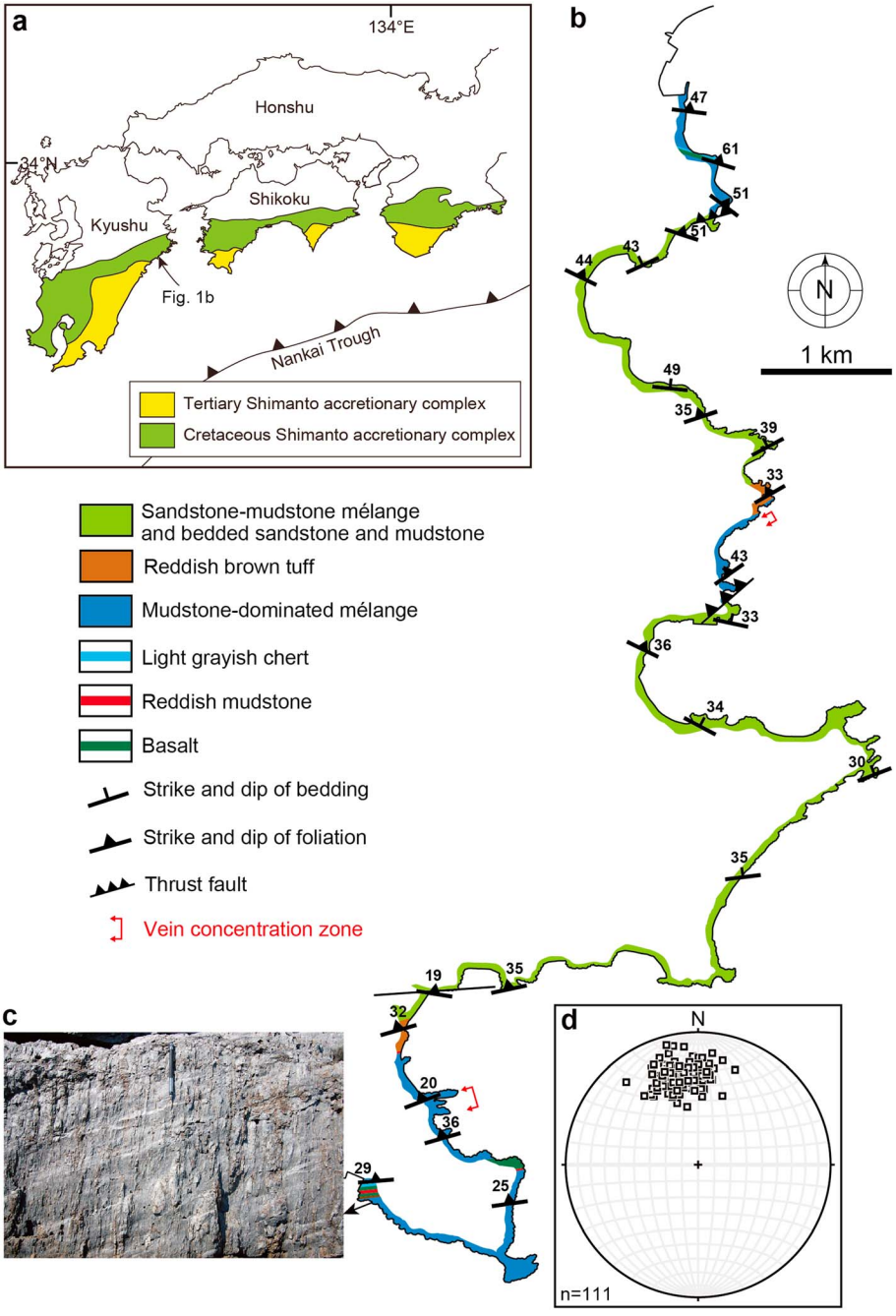

Figure 1. The Makimine mélange in the Shimanto accretionary complex. (a) Distribution of the Shimanto accretionary complex in southwest Japan. (b) Geological map of the Makimine mélange along the east coast of Kyushu. The location of the map is shown in Figure 1a. (c) Stretching lineations developed on the surface of mélange foliation. The pencil is parallel to NNW-SSE oriented stretching lineations. The brighter bands represent intersection between foliation and kink bands. (d) Lower hemisphere equal-area stereoplots showing orientation of stretching lineations in the mélange.

3. Crack-Seal Veins and Viscous Shear Zones in Subduction Mélange

A 10 to 60-m-thick zone where quartz veins are highly concentrated occurs in the lower part of the Makimine mélange, within which a penetrative foliation is defined by pressure solution cleavage (Figure 1b). Along-strike continuity and across-strike structural repetition of the vein concentration zone, and no spatial correlation between the vein distribution zone and the thrust accommodating underplating, indicate that the zone of vein concentration was formed during subduction and prior to the underplating that incorporated the

mélange into the overlying accretionary prism (Figure 1b). Shear veins, foliation-parallel extension veins, subvertical extension veins, and viscous shear zones are recognized within the vein concentration zone (Figure 2).

Shear veins are subparallel to the mélange foliation, with along-strike length ranging from 1 to 10 m (typically about 1 m; Figures 2a and 3a). Shear veins are laminated and fibrous (Figure 2b), representing multiple episodes of dilation and quartz precipitation along shear surfaces. The internal texture of shear veins is characterized by crack-seal texture defined by phyllosilicate inclusion bands subparallel to vein margins, with spacing ranging from 20 to 38 μm (Figure 2c and supporting information). At dilational stepovers, the inclusion bands are oblique to vein margins, and slip increments determined from fiber growth increments are 0.1–0.2 mm (Figure 2d). On the basis of the dip direction of inclusion bands at dilational stepovers and steps on the vein surfaces, shear veins exhibit thrust shear sense (Figures 2b and 2d). Slickenfiber orientations are consistent with the top-SSE shear direction determined from the trend of stretching lineations (Figures 1d and 3a). Tectonic reconstructions indicate subduction toward the NNW (Müller et al., 2008; Whittaker et al., 2007), consistent with top-SSE shear, and thus, the kinematics of both stretching lineations and localized, frictional shear veins are compatible with low-angle thrust faulting during subduction.

Foliation-parallel extension veins also show crack-seal texture marked by development of inclusion bands of ~28 to 42-μm spacing but lack dilational stepovers and slickenfibers on vein surfaces (Figure 2a). The length of foliation-parallel extension veins along strike is typically ~1 m, similar to that of shear veins. Subvertical extension veins are straight or sigmoidal, commonly constituting localized en echelon arrays (Figure 2e). Quartz crystals within the subvertical veins are elongate with long axes perpendicular to vein margins (Figure 2f), and a crack-seal texture is defined by 25-μm spaced inclusion bands aligned parallel to vein boundaries. Viscous shear zones are defined by <10-m-thick zones of rotated mélange foliations (Figure 2g). The viscous deformation is accommodated by pressure solution creep, illustrated by dark selvages and precipitates in pressure shadows, and commonly shows thrust shear sense. Some shear veins, subhorizontal extension veins, and subvertical extension veins cut the asymmetric fabric formed by viscous shear (Figure 2h) but are also themselves viscously deformed (Figure 2g). These features indicate that brittle shear slip with tensile fracturing and viscous shear occurred contemporaneously.

4. Low-Angle Thrust Faulting Under Tensile Overpressure

Pressure solution cleavage forms perpendicular to the greatest principal compressive stress (σ_1), and thus, the low-angle foliation implies a subvertical σ_1, consistent with subvertical extension veins. However, this foliation reflects finite strain and may therefore reflect long-term subvertical shortening, rather than stresses driving fracturing (e.g., Fagereng, 2013; Fisher & Byrne, 1987; Ujiie, 2002). It is conceivable that σ_1 was consistently subvertical and foliation-parallel extension veins involved opening of low cohesion, weak planes. However, this interpretation becomes problematic because (1) it requires σ_1 to become tensile and (2) it is difficult to explain the gentle dip of crack-seal bands within shear veins and foliation-parallel extension veins. We therefore suggest that the stress repeatedly rotated, which resulted in subvertical extension veins and foliation-parallel extension veins formed in different stress fields. As pointed out by Meneghini and Moore (2007), both explanations above require cyclicity in effective normal stress.

A very small angle (~5.5°) between the average orientations of shear veins and foliation-parallel extension veins indicates that shear veins were formed as hybrid extensional-shear fractures under low differential stress of $4T_0 < \Delta\sigma < 5.66\ T_0$ (Secor, 1965), where T_0 is the rock tensile strength and $\Delta\sigma$ is the differential stress (Figures 3a–3c). This is consistent with that shear veins opened at a high angle to the vein margin (Figure 2c). The geometrical relation between shear veins and foliation-parallel extension veins may represent fault-fracture meshes developed in a compressional regime (Sibson, 2017), where thrust faults lie at very low angles to σ_1, and the least principal compressive stress (σ_3) is approximately equal to the vertical stress (σ_V; Figure 3d). Under such a compressional regime, shear veins and hydraulic extension veins are expected to develop at near-lithostatic and supralithostatic fluid overpressures, respectively, as a result of opening directions of subhorizontal tensile veins being subparallel to the subvertical σ_3. Supposing T_0 = 1 MPa, a low estimate for typical pelitic rocks (Lockner, 1995) to account for the deformed nature of mélange mudstones, shear strength (τ) at a very low angle to σ_1 (5.5°) is extremely low, $0.38 < \tau < 0.54$ MPa. In this model, the mutually crosscutting relationship between the shear veins and local arrays of subvertical tensile veins, as well as the presence of stylolites and folded phyllosilicate inclusion bands in shear veins (Figure 2d),

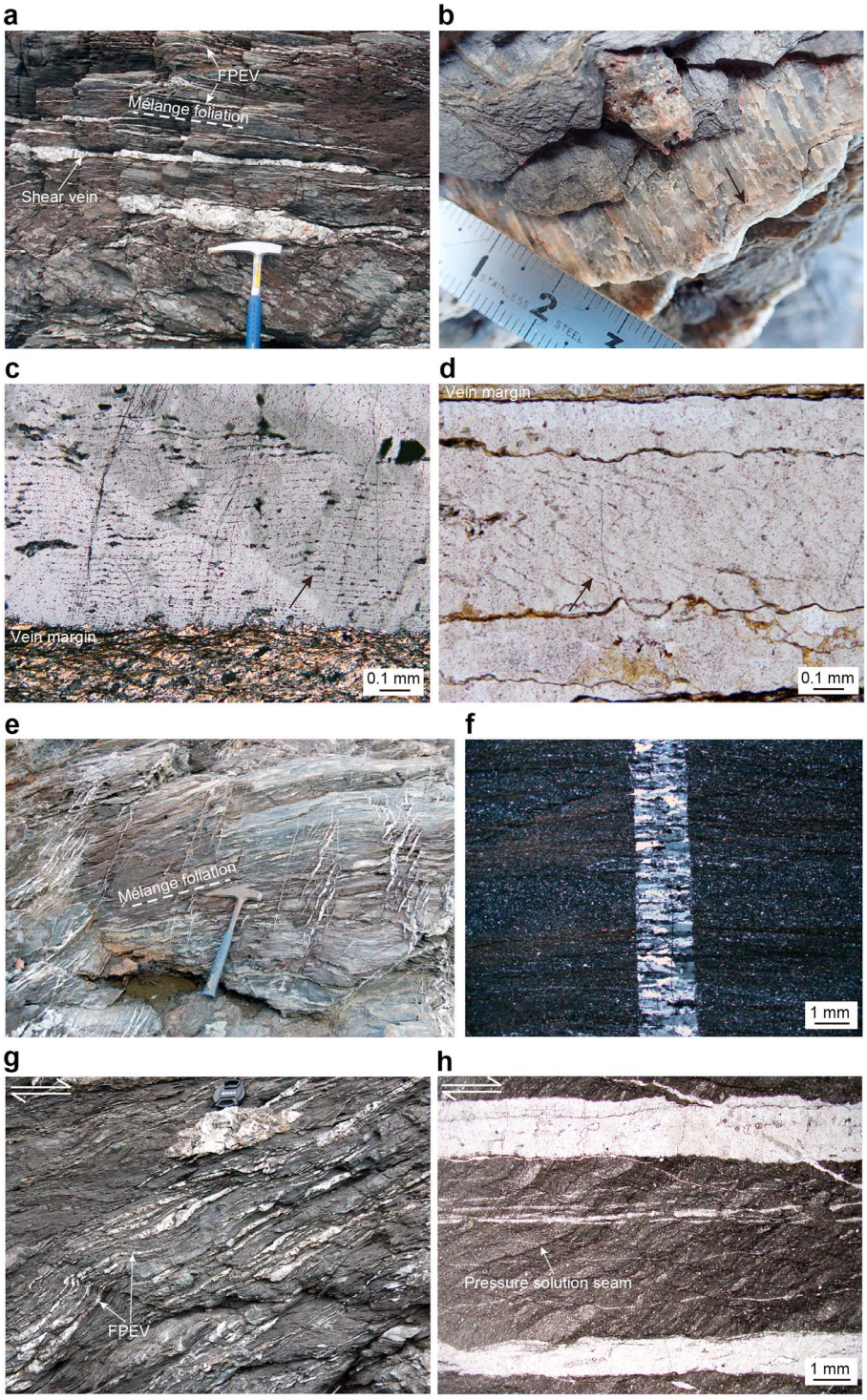

Figure 2. Representative deformation in subduction mélange. The half arrows indicate sense of shear. FPEV, foliation-parallel extension veins. (a) Macroscopic appearance of a shear vein and FPEV along the strike. (b) Slikenfibers and step (black arrow) developed on the surface of shear vein, showing thrust sense of shear. (c) Microscopic appearance of a shear vein cut parallel to slickenfibers and perpendicular to the shear surface under cross-polarized light, showing repeated episodes of cracking and sealing. The near-parallelism between phyllosilicate inclusion bands (black arrow) and the vein margin indicates that the shear vein open at a high angle to the vein margin, representing a hybrid extensional-shear fracture. (d) Folded phyllosilicate inclusion bands (black arrow) at dilational stepovers under plane-polarized light. The horizontal dark lines represent stylolites. (e) Macroscopic appearance of subvertical extension veins along the dip showing en echelon arrays. (f) Microscopic appearance of a subvertical extension vein under cross-polarized light. (g) Macroscopic appearance of a viscous shear zone along the dip showing thrust sense of shear. (h) Microscopic appearance of a viscous shear zone under plane-polarized light, showing the development of asymmetric pressure solution fabric cut by subhorizontal extension veins.

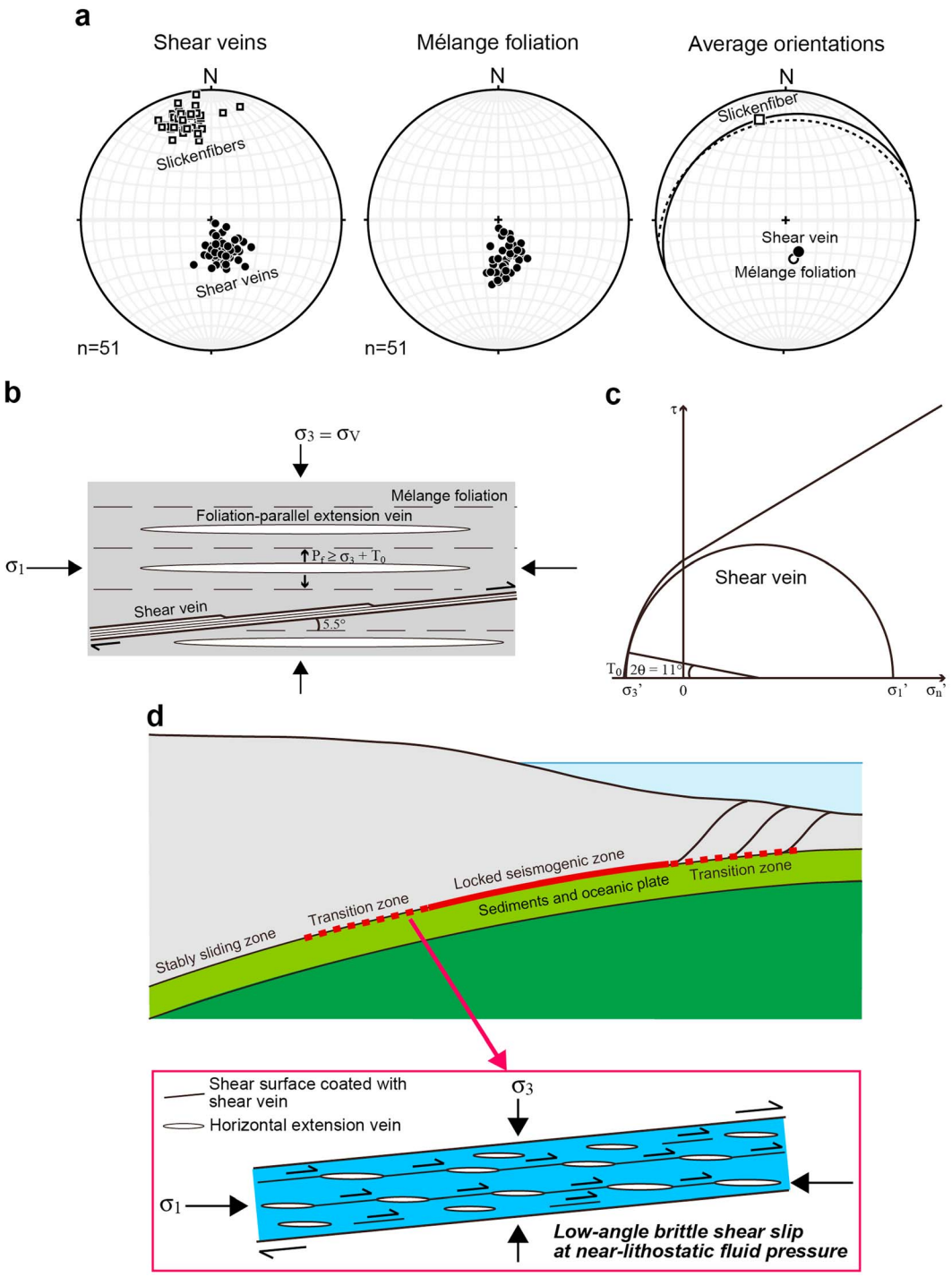

Figure 3. Low-angle thrust faulting at a very low angle to σ_1 under tensile overpressure. (a) Lower hemisphere equal-area stereoplots showing orientation of slickenfiber shear veins, mélange foliation, and average orientations of slickenfiber shear veins and mélange foliation in the vein concentration zone in the lower thrust sheet. (b) Schematic of geometrical relation between shear veins and foliation-parallel extension veins in a compressional regime with $\sigma_3 = \sigma_V$. (c) Mohr diagram showing conditions of a hybrid extensional-shear fracture at a very low angle to σ_1. τ, shear stress; σ_n', effective normal stress. (d) Schematic of fault-fracture meshes developed along the subduction plate boundary.

implies that the local stress field could transiently swap between vertical σ_3 and vertical σ_1, which is also indicative of low differential stress. If, like Fagereng et al. (2011), we assume a low shear modulus of 3 GPa for the mélange rocks, the stress drop for 0.1 to 0.2-mm slip increments on 1 to 10-m long faults is 30–600 kPa, consistent with very low driving stresses.

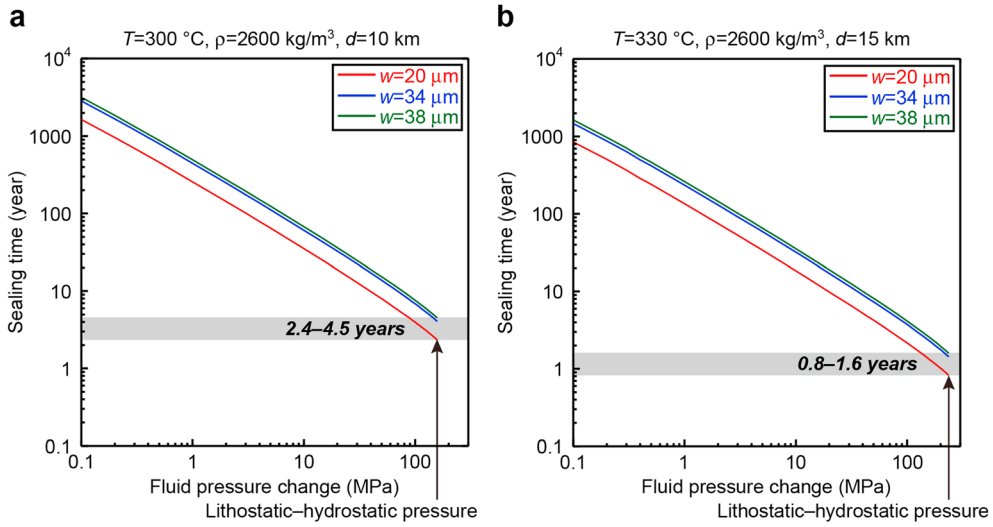

Figure 4. Sealing time for the width (*w*) of inclusion bands in quart-filled shear veins. (a) At depth of 10 km and temperature of 300°C. (b) At depth of 15 km and temperature of 330°C.

The observations and model presented here differ in geometry from that described by Fagereng et al. (2011). The vein system they describe, in the Chrystalls Beach Complex, New Zealand, consistently shows coeval shear and extension veins formed under a subvertical σ_1. The steep σ_1 determined in the Chrystalls Beach Complex is typical of weak, underthrust sediments (e.g., Fisher & Byrne, 1987), consistent also with thrust faults there developed along weak, low cohesion, clay-rich cleavage (Fagereng et al., 2010). In the Makimine mélange, a horizontal σ_1 explains many of the brittle structures, but episodically, the stress field switched to vertical σ_1. This may be a dynamic effect, as also seen in focal mechanisms before and after the 2011 Tohoku-Oki earthquake (e.g., Hasegawa et al., 2011, Lin et al., 2013). Why the dominant stress field differs between Chrystalls Beach mélange and Makimine mélange shear veins is unclear, but it may relate to differences in the frictional strength of the fault surfaces or the bulk rheology of the mélanges. In both cases, however, thrust sense faulting occurred episodically at low differential stress and near-lithostatic fluid pressure.

5. Time Interval Between Crack-Seal Events

The crack-seal textures in shear and extension veins indicate that discontinuous deformation occurred repeatedly, and we interpret the repetition to correlate with temporal fluid pressure variations. To investigate the time required between each crack-seal event, a kinetic model for quartz precipitation (Rimstidt & Barnes, 1980), driven by movement of fluid down a pressure gradient, was applied for quartz-filled shear veins (supporting information). The model considers the width of inclusion bands in shear veins (20–38 μm), the typical length of shear veins (1 m), fluid pressure reduction at the start of each crack-seal event, and ambient temperature of 300–330°C (supporting information). Assuming that subhorizontal tensile fractures require at least lithostatic fluid pressures, and that opening of these fractures creates at least temporarily an interconnected fluid pathway, we consider a local fluid pressure change equal to lithostatic minus hydrostatic pressure at the time of fracture opening. At 10–15 km depth with average rock density of 2,600 kg/m^3, this is a fluid pressure drop of 157–235 MPa. This large fluid pressure drop is consistent with various vapor/liquid ratios in two-phase fluid inclusions within shear veins (supporting information). Assuming precipitation rate controls the time of healing (i.e., silica can be transported to the open fracture at least as far as quartz precipitates), the veins can close in less than 1.6–4.5 years (Figure 4). Quartz crystals are blocky and do not show collapse structures, which is consistent with precipitation in an open crack that did not collapse. This lack of collapse structures may be surprising upon a large fluid pressure drop but could possibly be explained by relatively fast precipitation from fluids moving through the fracture system in response to increased fracture permeability (cf. Vrolijk, 1987). On the other hand, we note that the large fluid pressure drop may have limited crack propagation and locally arrested shear displacement. We thus assume that this ≤1.6 to 4.5-year estimate corresponds to minimum healing time between deformation events. If the fluid temperature is

higher than ambient temperature, the model suggests that healing time becomes shorter, and similarly, if precipitation is coupled to collapse of pore space under increasing effective normal stress, healing rates will also increase (Rimstidt & Barnes, 1980).

6. Discussion and Conclusion

Our results show that shear veins in subduction mélange record low-angle thrust faulting at very small shear strength and near-lithostatic fluid overpressures, consistent with plate boundary shear kinematics and key geophysical observations of slow earthquakes in subduction zones. The time required between discrete vein opening events, assuming complete healing of cracks defined by inclusion band spacing, gives a constraint of $\leq$1.6–4.5 years for the minimum time interval of repeated thrust faulting events. This repeat time is comparable to recurrence intervals of slow earthquakes. A large number (~100–150) of inclusion bands in shear veins (supporting information) indicate multiple occurrences of fracturing under elevated fluid pressure and subsequent restoration of cohesive and tensile strength through hydrothermal precipitation. If the slip increment of ~0.1–0.2 mm at dilational stepovers corresponds to the shear displacement during a single slow earthquake, ~100–150 inclusion bands suggest that cumulative displacement along individual low-angle thrust faults is ~0.01–0.03 m. Alternatively, the total displacement during a single slow earthquake event may be distributed into many different shear surfaces. In this case, the slip increment of ~0.1–0.2 mm during one crack-seal event could accommodate a small component of the total displacement during that slow earthquake. Crack-seal shear and extension veins are also recognized in other mélanges and metamorphic rocks exhumed from the source depths of slow earthquakes (Fagereng et al., 2011; Fisher & Brantley, 2014; Sibson, 2017). Such crack-seal veins may also record repeated slow earthquake events.

In the Makimine mélange, the intensely veined zone is tens of meters thick and involves a combination of viscous and frictional deformations. Such frictional-viscous deformation zones that are narrower than the full width of a mélange shear zone have been reported from other exhumed subduction zones, irrespective of deformation mechanisms of pressure solution creep or dislocation creep (Fagereng et al., 2014; Rowe et al., 2013). Within a mélange shear zone, frictional-viscous deformation along narrow zones could represent deformation at higher strain rates. The absence of geological evidence of frictional heat (e.g., pseudotachylytes) in narrow shear zones suggests that strain rate is slower than seismic slip rate. Therefore, if localization of viscous shear into narrow zones implies higher strain rates (cf. Fagereng et al., 2014), then these may be candidates for slow earthquake zones. A common feature is coexistence of mineralized veins and relatively intense viscous fabrics, implying locally elevated fluid pressures and increased viscous strains, respectively. The geophysically observed signature of such deformation may be transient slow slip faster than plate motion rates (SSEs) accompanied by localized frictional failure (tremor containing LFEs).

Acknowledgments
This work is supported by the Japan Society for the Promotion of Science KAKENHI grant JP16H06476. A.F. is supported by ERC Starting Grant 715836 "MICA." Structural, Raman, and fluid inclusion data and parameters and values used in the kinetic modeling are available in the supplementary materials. J. Kirkpatrick and an anonymous reviewer provided valuable comments that significantly improved the manuscript. We thank GRL Editor Lucy Flesch for evaluation of the paper. We would also like to thank K. Ohta, Y. Yamashita, S. Katakami, and Y. Ito for valuable discussions.

References

Akinfiev, N. N., & Diamond, L. W. (2009). A simple predictive model of quartz solubility in water-salt-CO_2 systems at temperatures up to 1000°C and pressures up to 1000 MPa. *Geochimica et Cosmochimica Acta*, *73*(6), 1597–1608. https://doi.org/10.1016/j.gca.2008.12.011

Araki, E., Saffer, D. M., Kopf, A. J., Wallace, L. M., Kimura, T., Machida, Y., et al. (2017). Recurring and triggered slow-slip events near the trench at the Nankai Trough subduction megathrust. *Science*, *356*(6343), 1157–1160. https://doi.org/10.1126/science.aan3120

Behr, W. M., Kotowski, A. J., & Ashley, K. T. (2018). Dehydration-induced rheological heterogeneity and the deep tremor source in warm subduction zones. *Geology*, *46*, 475–478. https://doi.org/10.1130/G40105.1

Beroza, G. C., & Ide, S. (2011). Slow earthquakes and nonvolcanic tremor. *Annual Review of Earth and Planetary Sciences*, *39*(1), 271–296. https://doi.org/10.1146/annurev-earth-040809-152531

Fagereng, A. (2013). On stress and strain in a continuous-discontinuous shear zone undergoing simple shear and volume loss. *Journal of Structural Geology*, *50*, 44–53. https://doi.org/10.1016/j.jsg.2012.02.016

Fagereng, A., Hillary, G. W. B., & Diener, J. F. A. (2014). Brittle-viscous deformation, slow slip, and tremor. *Geophysical Research Letters*, *41*, 4159–4167. https://doi.org/10.1002/2014GL060433

Fagereng, A., Remitti, F., & Sibson, R. H. (2010). Shear veins observed within anisotropic fabric at high angles to the maximum compressive stress. *Nature Geoscience*, *3*(7), 482–485. https://doi.org/10.1038/ngeo898

Fagereng, A., Remitti, F., & Sibson, R. H. (2011). Incrementally developed slickenfibres—geological record of repeating low stress-drop seismic events. *Tectonophysics*, *510*(3-4), 381–386. https://doi.org/10.1016/j.tecto.2011.08.015

Fisher, D., & Byrne, T. (1987). Structural evolution of underthrusted sediments, Kodial Island, Alaska. *Tectonics*, *6*, 775–793. https://doi.org/10.1029/TC006i006p00775

Fisher, D. M., & Brantley, S. L. (2014). The role of silica redistribution in the evolution of slip instabilities along subduction interfaces: Constraints from the Kodiak accretionary complex, Alaska. *Journal of Structural Geology*, *69*, 395–414. https://doi.org/10.1016/j.jsg.2014.03.010

Hara, H., & Kimura, K. (2008). Metamorphic and cooling history of the Shimanto accretionary complex, Kyushu, southwest Japan: Implications for the timing of out-of-sequence thrusting. *Island Arc*, *17*(4), 546–559. https://doi.org/10.1111/j.1440-1738.2008.00636.x

Hasegawa, A., Yoshida, K., & Okada, T. (2011). Nearly complete stress drop in the 2011 M_w 9.0 off the Pacific coast of Tohoku earthquake. *Earth, Planets and Space*, *69*, 703–707.

Hayman, N. W., & Lavier, L. L. (2014). The geological record of deep episodic tremor and slip. *Geology*, *42*(3), 195–198. https://doi.org/10.1130/G34990.1

Ide, S., Shelly, D. R., & Beroza, G. C. (2007). Mechanism of deep low frequency earthquakes: Further evidence that deep non-volcanic tremor is generated by shear slip on the plate interface. *Geophysical Research Letters*, *34*, L03308. https://doi.org/10.1029/2006GL028890

Kagi, H., Tsuchida, I., Wakatsuki, M., Takahashi, K., Kamimura, N., Iuchi, K., & Wada, H. (1994). Proper understanding of down-shifted Raman spectra of natural graphite: Direct estimation of laser-induced rise in sample temperature. *Geochimica et Cosmochimica Acta*, *58*(16), 3527–3530. https://doi.org/10.1016/0016-7037(94)90104-X

Kouketsu, Y., Mizukami, T., Mori, H., Endo, S., Aoya, M., Hara, H., et al. (2014). A new approach to develop the Raman carbonaceous material geothermometer for low-grade metamorphism using peak width. *Island Arc*, *23*(1), 33–50. https://doi.org/10.1111/iar.12057

Lahfid, A., Beyssac, O., Deville, E., Negro, F., Chopin, C., & Goffé, B. (2010). Evolution of the Raman spectrum of carbonaceous material in low-grade metasediments of the Glarus Alps (Switzerland). *Terra Nova*, *22*(5), 354–360. https://doi.org/10.1111/j.1365-3121.2010.00956.x

Lin, W., Conin, M., Moore, J. C., Chester, F. M., Nakamura, Y., Mori, J. J., et al. (2013). Stress state in the largest displacement area of the 2011 Tohoku-Oki earthquake. *Science*, *339*(6120), 687–690. https://doi.org/10.1126/science.1229379

Lockner, D. A. (1995). *Rock physics and phase relations, a handbook of physical constants* (pp. 127–147). Washington, DC: American Geophysical Union.

Mackenzie, J. S., Needham, D. T., & Agar, S. M. (1987). Progressive deformation in an accretionary complex: An example from the Shimanto belt of eastern Kyushu, southwest Japan. *Geology*, *15*(4), 353–356. https://doi.org/10.1130/0091-7613(1987)15<353:PDIAAC>2.0.CO;2

Meneghini, F., & Moore, J. C. (2007). Deformation and hydrofracture in a subduction thrust at seismogenic depths: The Rodeo Cove thrust zone, Marin Headlands, California. *GSA Bulletin*, *119*(1-2), 174–183. https://doi.org/10.1130/B25807.1

Müller, R. D., Sdrolias, M., Gaina, C., Steinberger, B., & Heine, C. (2008). Long-term sea-level fluctuations driven by ocean basin dynamics. *Science*, *319*(5868), 1357–1362. https://doi.org/10.1126/science.1151540

Nakano, M., Hori, T., Araki, E., Kodaira, S., & Ide, S. (2018). Shallow very-low-frequency earthquakes accompany slow slip events in the Nankai subduction zone. *Nature Communications*, *9*(1), 984. https://doi.org/10.1038/s41467-018-03431-5

Obara, K., Hirose, H., Yamamizu, F., & Kasahara, K. (2004). Episodic slow slip events accompanied by non-volcanic tremors in southwest Japan subduction zone. *Geophysical Research Letters*, *31*, L23602. https://doi.org/10.1029/2004GL020848

Obara, K., & Kato, A. (2016). Connecting slow earthquakes to huge earthquakes. *Science*, *353*(6296), 253–257. https://doi.org/10.1126/science.aaf1512

Okamoto, A., Saishu, H., Hirano, N., & Tsuchiya, N. (2010). Mineralogical and textural variation of silica minerals in hydrothermal flow-through experiments: Implications for quartz vein formationm. *Geochimica et Cosmochimica Acta*, *74*(13), 3692–3706. https://doi.org/10.1016/j.gca.2010.03.031

Okamoto, A., & Sekine, K. (2011). Textures of syntaxial quartz veins synthesized by hydrothermal experiments. *Journal of Structural Geology*, *33*(12), 1764–1775. https://doi.org/10.1016/j.jsg.2011.10.004

Palazzin, G., Raimbourg, H., Famin, V., Jolivet, L., Kusaba, Y., & Yamaguchi, A. (2016). Deformation processes at the down-dip limit of the seismogenic zone: The example of Shimanto accretionary complex. *Tectonophysics*, *687*, 28–43. https://doi.org/10.1016/j.tecto.2016.08.013

Peng, Z., & Gomberg, J. (2010). An integrated perspective of the continuum between earthquakes and slow slip phenomena. *Nature Geoscience*, *3*(9), 599–607. https://doi.org/10.1038/ngeo940

Rimstidt, J. D., & Barnes, H. L. (1980). The kinetics of silica-water reactions. *Geochimica et Cosmochimica Acta*, *44*(11), 1683–1699. https://doi.org/10.1016/0016-7037(80)90220-3

Rogers, G., & Dragert, H. (2003). Episodic tremor and slip on the Cascadia subduction zone: The chatter of silent slip. *Science*, *300*(5627), 1942–1943. https://doi.org/10.1126/science.1084783

Rowe, C. D., Moore, J. C., Remitti, F., & the IODP Expedition 343/343T Scientists (2013). The thickness of subduction plate boundary faults from the seafloor into the seismogenic zone. *Geology*, *41*(9), 991–994. https://doi.org/10.1130/G34556.1

Saffer, D. M., & Wallace, L. M. (2015). The frictional, hydrological, metamorphic and thermal habitat of shallow slow earthquakes. *Nature Geoscience*, *8*(8), 594–600. https://doi.org/10.1038/ngeo2490

Schwartz, S. Y., & Rokosky, J. M. (2007). Slow slip events and seismic tremor at circum-pacific subduction zones. *Reviews of Geophysics*, *45*, RG3004. https://doi.org/10.1029/2006RG000208

Secor, D. T. (1965). Role of fluid pressure in jointing. *American Journal of Science*, *263*(8), 633–646. https://doi.org/10.2475/ajs.263.8.633

Shelly, D. R., Beroza, G. C., & Ide, S. (2007). Non-volcanic tremor and low-frequency earthquakes swarms. *Nature*, *446*(7133), 305–307. https://doi.org/10.1038/nature05666

Sibson, R. H. (2017). Tensile overpressure compartments on low-angle thrust faults. *Earth, Planets and Space*, *69*(1), 113. https://doi.org/10.1186/s40623-017-0699-y

Skarbek, R. M., Rempel, A. W., & Schmidt, D. A. (2012). Geologic heterogeneity can produce aseismic slip transients. *Geophysical Research Letters*, *39*, L21306. https://doi.org/10.1029/2012GL053762

Ujiie, K. (2002). Evolution and kinematics of an ancient décollement zone, mélange in the Shimanto accretionary complex of Okinawa Island, Ryukyu Arc. *Journal of Structural Geology*, *24*(5), 937–952. https://doi.org/10.1016/S0191-8141(01)00103-1

Ujiie, K., & Kimura, G. (2014). Earthquake faulting in subduction zones: Insights from fault rocks in accretionary prisms. *Progress in Earth and Planetary Science*, *1*(1), 7–30. https://doi.org/10.1186/2197-4284-1-7

Ujiie, K., Yamaguchi, H., Sakaguchi, A., & Toh, S. (2007). Pseudotachylytes in an ancient accretionary complex and implications for melt lubrication during subduction zone earthquakes. *Journal of Structural Geology*, *29*(4), 599–613. https://doi.org/10.1016/j.jsg.2006.10.012

Vrolijk, P. (1987). Tectonically driven fluid flow in the Kodiak accretionary complex, Alaska. *Geology*, *15*(5), 466–469. https://doi.org/10.1130/0091-7613(1987)15<466:TDFFIT>2.0.CO;2

Wallace, L. M., Webb, S. C., Ito, Y., Mochizuki, K., Hino, R., Henrys, S., et al. (2016). Slow slip near the trench at the Hikurangi subduction zone, New Zealand. *Science*, *352*(6286), 701–704. https://doi.org/10.1126/science.aaf2349

Whittaker, J. M., Muller, R. D., Leitchenkov, G., Stagg, H., Sdrolias, M., Gaina, C., & Goncharov, A. (2007). Major Australian-Antarctic plate reorganization at Hawaiian-Emperor bend time. *Science*, *318*(5847), 83–86. https://doi.org/10.1126/science.1143769

Yamashita, Y., Yakiwara, H., Asano, Y., Shimizu, H., Uchida, K., Hirano, S., et al. (2015). Migrating tremor off southern Kyushu as evidence for slow slip of a shallow subduction interface. *Science*, *348*(6235), 676–679. https://doi.org/10.1126/science.aaa4242